**Earthquakes and Structures**, *Vol. 7, No. 5 (2014) 667-689*
DOI: http://dx.doi.org/10.12989/eas.2014.7.5.667 

# Comparative in-plane pushover response of a typical RC rectangular wall designed by different standards

Farhad Dashti*, Rajesh P Dhakal[a] and Stefano Pampanin[b]

*Department of Civil and Natural Resources Engineering, University of Canterbury, Private Bag 4800, Christchurch 8140, New Zealand*

*(Received February 28, 2014, Revised May 5, 2014, Accepted May 8, 2014)*

**Abstract.** Structural walls (also known as shear walls) are one of the common lateral load resisting elements in reinforced concrete (RC) buildings in seismic regions. The performance of RC structural walls in recent earthquakes has exposed some problems with the existing design of RC structural walls. The main issues lie around the buckling of bars, out-of plane deformation of the wall (especially the zone deteriorated in compression), reinforcement getting snapped beneath a solitary thin crack etc. This study compares performance of a typical wall designed by different standards. For this purpose, a case study RC shear wall is taken from the Hotel Grand Chancellor in Christchurch which was designed according to the 1982 version of the New Zealand concrete structures standard (NZS3101:1982). The wall is redesigned in this study to comply with the detailing requirements of three standards; ACI-318-11, NZS3101:2006 and Eurocode 8 in such a way that they provide the same flexural and shear capacity. Based on section analysis and pushover analysis, nonlinear responses of the walls are compared in terms of their lateral load capacity and curvature as well as displacement ductilities, and the effect of the code limitations on nonlinear responses of the different walls are evaluated. A parametric study is also carried out to further investigate the effect of confinement length and axial load ratio on the lateral response of shear walls.

**Keywords:** reinforced concrete; shear wall; design codes; comparative performance; cnfinement length; axial load ratio

## 1. Introduction

Structural wall systems were introduced in the 1970s, and design provisions for this system have evolved since then. Barbell-shaped wall sections with boundary elements protruding from the surface of the wall were more common in the 1970s and 1980s. In this system, the boundary elements acted as columns resisting axial load and overturning. In recent years, as the optimization issues have gained importance, slender rectangular walls which take less space and are believed to be more economical designs have become more common in many countries like New Zealand. Use of higher concrete strengths has also resulted in more slender profiles than have been

*Corresponding author, Ph.D. Student, E-mail: farhad.dashti@pg.canterbury.ac.nz
[a]Professor, E-mail: rajesh.dhakal@canterbury.ac.nz
[b]Professor, E-mail: stefano.pampanin@canterbury.ac.nz


http://www.techno-press.org/?journal=eas&subpage=7 ISSN: 2092-7614 (Print), 2092-7622 (Online)

previously tested in the laboratory or in real buildings under earthquakes. Slender walls with nominal reinforcing and higher axial load have failed in recent earthquakes in brittle shear-compression mode or by premature fracture of tensile/compressive reinforcing bars (Wallace 2012, Wallace and Moehle 2012).

RC buildings in New Zealand can be classified into two categories; namely Pre- 1970 buildings which were designed prior to the 1976 revision of the RC seismic design code, NZS4203:1976, and modern buildings that were designed using the 1976 or a later version of the RC seismic design code. Pre-1970s RC buildings generally have inadequate seismic capacity and are likely to experience brittle failure as they have deficiencies like lack of confinement in walls, joints and columns, inadequate reinforcing and anchorage details, poor material properties and use of plain reinforcing bars, no capacity design principles and irregular building configurations (Kam *et al*. 2011). According to the EERI special earthquake report on the M6.3 Christchurch, New Zealand, earthquake of February 22 (2011) and Canterbury Earthquakes Royal Commission Reports (CERC) (2012), structural walls did not perform as anticipated. Boundary zone crushing and bar buckling were observed mostly in Pre-1970s RC walls which were generally lightly reinforced, were not detailed for ductility and had inadequate reinforcement to provide confinement to the concrete and buckling restraint to the longitudinal reinforcement.

On the other hand, modern (Post-1970s) RC wall buildings were observed to have experienced failure patterns like wall web buckling, boundary zone bar fracture and buckling failure of ducted splice. In a number of cases, compression failure occurred in the outstanding legs of T and L walls in addition to significant out-of-plane displacements, thereby resulting in overall buckling of the wall. In some cases, the transverse reinforcement did not meet the spacing requirement to prevent buckling of the longitudinal reinforcement, and bar buckling resulted in high localized strains and decreased the tensile strain capacity. Figs. 1-2 show some examples of different failure modes, observed in RC walls in 2011 Christchurch earthquake.

As a result of the performance of the shear walls in recent earthquakes in New Zealand, some issues have been identified to be further investigated (NZRC 2012). The reinforcement ratio and arrangement turned out to be inadequate in some of the damaged walls and resulted in formation of a single primary crack. The reinforcement ratio should ensure extended yielding beyond the vicinity of a single crack. This issue can be sorted out by using higher minimum reinforcement ratio, changing distribution of the reinforcement and de-bonding bars in the critical zones (NZRC 2012). Also, there are some issues that considerably affected the performance of structural walls in buildings. For instance, some walls sustained greater axial forces than were anticipated in the design due to the fact that as reinforcement yielding and formation of plastic hinge started in the wall, other structural elements provided restraint against elongation of the wall and resulted in considerable increase in the axial load ratio.

Compression yielding of the vertical reinforcement in unconfined region of the wall can result in buckling. In other words, if the provided confinement length is not enough to cover the whole compression area of the wall where axial compressive strain can be considerably beyond the yield point of steel and crushing strain of concrete, vertical reinforcement of the unconfined zone may undergo big strains and cause sudden degradation in overall response of the wall.

The effect of bi-directional loading on walls has received little attention from researchers, and most wall experiment results used to establish design provisions tested response of the walls under in-plane loading only. In some damaged walls like the one in the Christchurch Grand Chancellor Hotel building, out of plane failure of the wall at the base was observed, which could have been

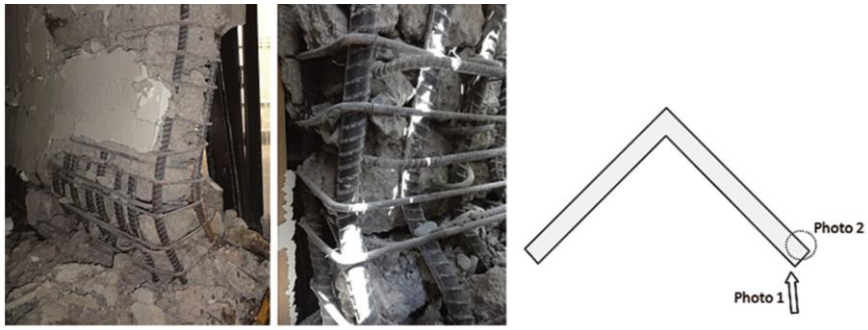


Fig. 1 Web buckling of well-confined wall (Elwood 2013)

(a) (b)

Fig. 2 (a) Bar buckling and fracture in lightly reinforced slender RC shear wall; (b) Slender wall shear-axial failure (Kam *et al*. 2011)

triggered by ground motions in the out of plane direction.

Another issue that became a matter of concern in recent earthquakes in New Zealand (2011) and also in Chile (2010) was the slenderness ratio of walls for which suitable provisions are not provided in design codes to prevent buckling of walls subjected to moderate and high axial load ratios (Telleen *et al*. 2012a, Telleen *et al*. 2012b).

In this study, detailing requirements of reinforced concrete shear walls provided by different design codes are compared by designing a typical wall based on different standards and evaluating their performance. For this purpose, one of the RC shear walls damaged in the 2011 Christchurch earthquake was used for comparison. The wall is taken from the Christchurch Grand Chancellor Hotel which was severely damaged (requiring demolition) in the 22 February 2011 earthquake.

The proposed procedures for analytical modeling of an RC shear wall can be classified into two broad groups, microscopic and macroscopic models. Microscopic models are based on a detailed interpretation of the local behavior to obtain a solution through the finite element approach, whereas phenomenological macroscopic models are based on capturing overall behavior with reasonable accuracy. Micro models can provide a detailed prediction of the local behavior, but due to complexities involved in developing the model and interpreting the results, their implementation is not common for nonlinear analyses of multi-story buildings with RC shear walls which need a

large amount of time for preparing the structural model, computing the response, and interpretation of the results. Therefore, simplified models are usually used for capturing overall response of walls interacting with frames (Sullivan 2010). Recently, several approaches have been used for wall modeling using microscopic models (Wan and Li 2012, Boulanger *et al*. 2013, Luu *et al*. 2013, Song *et al*. 2013), and the research on macroscopic models is still in progress trying to come up with a model that can capture some of the main features of the wall response like shear-flexure interaction (Massone *et al*. 2009, Panagiotou *et al*. 2012).

In this study, a finite element model is adopted for push-over analysis of the wall models which is verified using cyclic experimental results of a flexure dominated wall specimen.

## 2. Comparative design

### *2.1 Case study wall*

The Hotel Grand Chancellor was one of the severely damaged buildings during the 22 February 2011 Christchurch earthquake. The tower was constructed between 1985 and 1988 according to the NZS4203:1984 loading standard and NZS3101:1982 concrete design standard, and was the tallest building in Christchurch at the time of construction. The hotel had a tower with 15 levels of accommodation above 12 half-levels of carparking (equivalent to 6 full floors) and reception in the ground floor. The tower had plan dimensions of approximately 33 m × 24 m. According to Dunning Thornton Report (2011), the Hotel Grand Chancellor has a calculated initial period (at yield of the tower frames) of around 2.8 seconds. As a structure yields it also softens and as a consequence the period lengthens. In a post-elastic scenario the effective period is calculated to be around 4 seconds. Also, based on the displacement spectrum captured for the 22 February 2011 earthquake, the maximum predicted displacement at effective center of mass and allowing for pile flexibility is reported as 500 mm (Dunning Thornton Report 2011). As the wall is extended up to level 14 only, displacement demand of the wall would be smaller.

As shown in Fig. 3, the lateral load resisting system comprised of RC shear walls in the lower tower and moment-resisting RC frames in the upper tower resulting in the vertical irregularity of the structure (Dunning Thornton Report 2011).The building had horizontal irregularity as well, arising from the cantilever bay between grids D and E. The east side of the building (bay D-E) was cantilevered over an adjacent service lane (Fig. 3). Several deep transfer girders were used between levels 12 and 14 to transfer the cantilever load to the adjacent lane leading to a considerably great amount of axial load applied to a critical shear wall denoted as D5-6 in Fig. 3.

According to Dunning Thornton Report (2011), Wall D5-6 was a doubly reinforced (two layers of reinforcing in each direction, horizontal and vertical) concrete cantilever shear wall that extended from the pilecap at ground floor to level 14. Typically its clear height between floors is approximately 2.4 m but between ground and first floor its clear height is approximately 5.1m. The wall has plan dimensions of 4.9 m × 0.4 m. The wall was relatively lightly reinforced (0.45% vertical) and had only nominal confinement reinforcing, ties and links, at each end of the wall. The wall had the potential to attract high axial (vertical) loads resulting from:

- Gravity loads from a contributing area of approximately 100 $m^2$ × 21 floors.
- Bi-directional seismic frame action (overstrength beam shears).

- Induced loads resulting from the shear loads attracted by the cantilever transfer beams between levels 12 and 14.
- Vertical seismic accelerations.

The wall also had the potential to attract moments and shear loads (in-plane and out-of-plane) in proportion to its stiffness and the relative displacement of the floors that it was connected to. Wall D5-6 naturally attracted extreme vertical actions compared to other shear walls in the building. There were three other, similar walls that also supported columns subject to bi-directional axial actions; the wall at D10-11 (Fig. 3) supported a similar floor area to D5-6 but it had a return wall to brace the highly loaded end. Its maximum unsupported height was also only 3.6m compared to 5.1m and only one of the transfer beams it carried was full depth between storeys. The wall at A10-11 (Fig. 3) supported only one quarter of the area that D5-6 supported, had a lower height and was not affected by the transfer beam action. The wall at A4-6 (Fig. 3) also supported only one quarter of the area that D5-6 supported and was not affected by the transfer beam action. This wall was also twice the length of D5-6.

As shown in Fig. 4, wall D5-6 suffered a brittle failure at the base with out-of-plane instability. The failure plane initiated at the top of the lap splice in the web vertical reinforcement. The confinement hoops opened allowing the longitudinal bars to deform with the shortening of the wall. This wall was subjected to excessive amount of axial load from the cantilever structure, the corner column of the upper tower perimeter moment frame and the vertical excitation of the cantilever structures both above and below level 14. The combined axial load and bending exceeded the concrete compression strain capacity given the limited tie reinforcement provided at the base of the wall. Some out-of-plane drift of the wall during the earthquake excitation and the plane of weakness created at the end of the splice of the web vertical reinforcement further contributed to the failure at its base. Fig. 5 displays the reinforcement configuration of the wall along the length and height of the wall. Scrutinizing these details indicates a deficient confinement length and inadequate reinforcement ratio in the boundary element.

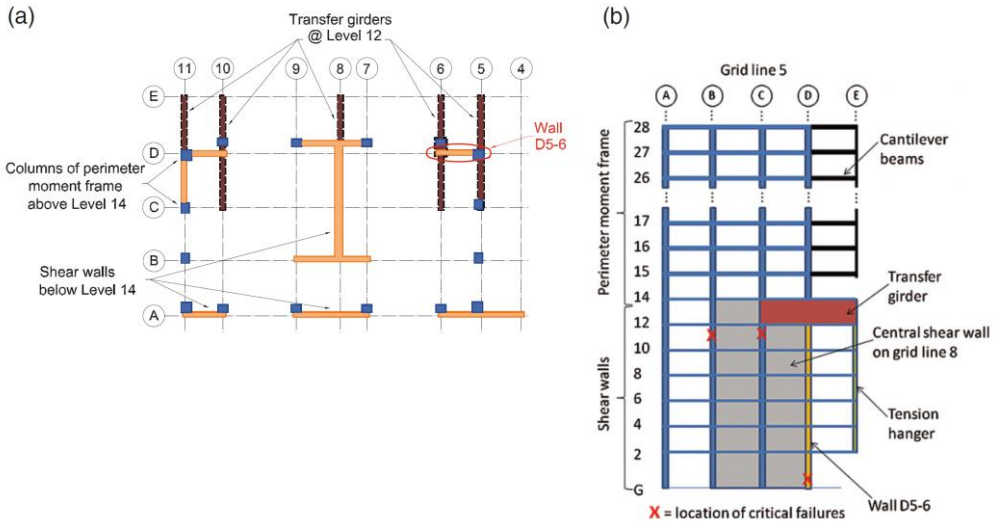


Fig. 3 Hotel grand chancellor structural layout sketch (a) plan; (b) elevation along grid line 5 (Elwood 2013)

Fig. 4 Failure of wall D5-6 (Kam *et al*. 2011)

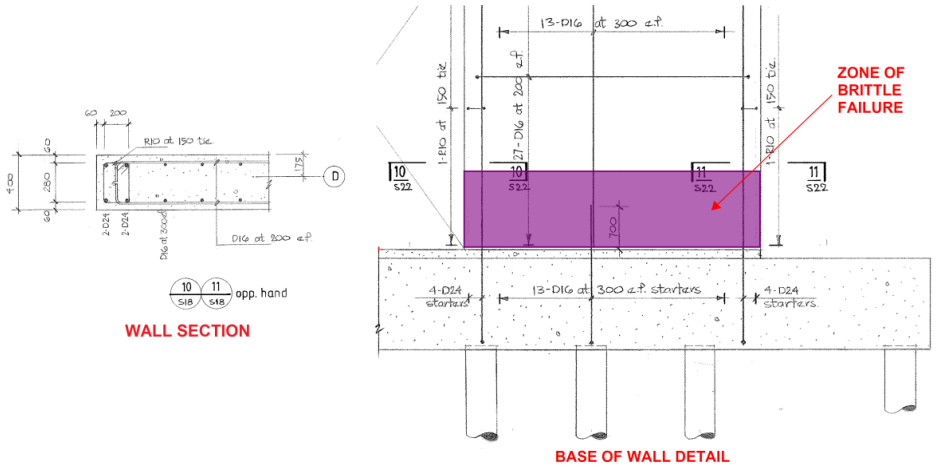


Fig. 5 Reinforcement details of wall D5-6 (Dunning Thornton Report 2011)

### *2.2 Modified design*

According to a consultancy report investigating into the performance of this wall (Dunning Thornton Report 2011), the original design actions of the wall are:

Axial Load = 17MN (0.25 $f_c$`Ag)
Moment = 8MN
Shear = 800kN

The wall is redesigned in this study to comply with the detailing requirements of three standards: ACI-318-11 (2011), NZS3101:2006 (2006) and Eurocode 8 (CEN 2004) in such a way that the demand used for design of the as-built wall (Wall D5-6) could be met. Fig. 6 displays the

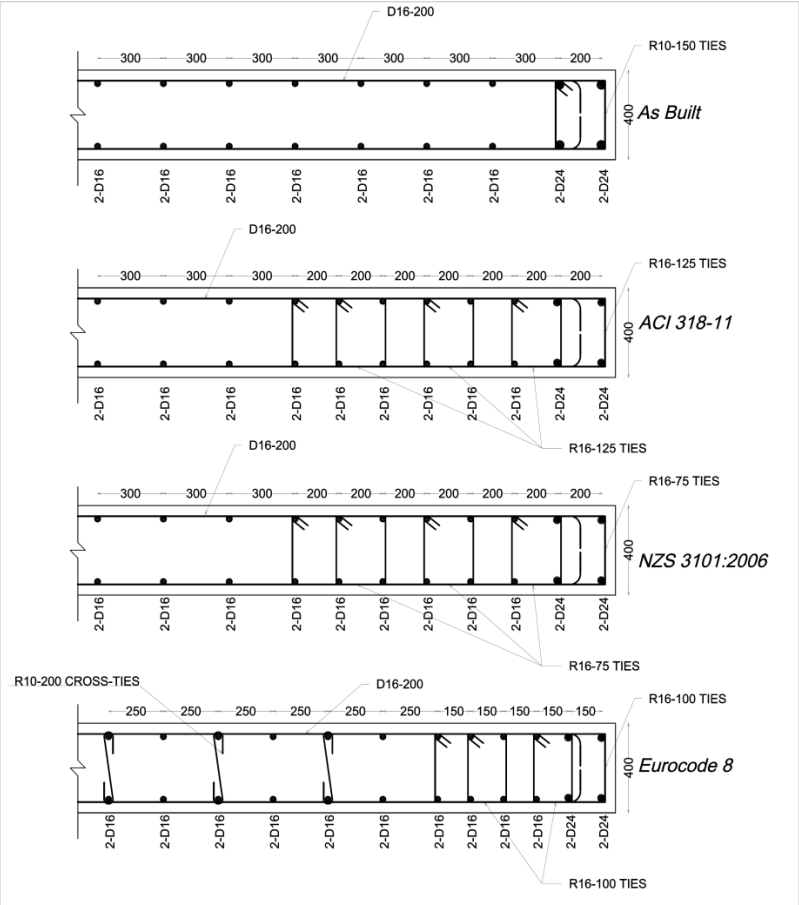


Fig. 6 Wall sections

wall sections designed based on the three codes in comparison with the as-built section. The as-built wall section was modified to meet the design requirements of each code with the least possible changes. As changes in reinforcement arrangement are unavoidable due to different detailing requirements, all walls were designed to satisfy the same strength demand.

Since ACI318-11 does not limit the web and boundary thickness of walls, the wall thickness was not changed. It should be noted that this issue is currently a matter of concern following the wall instabilities observed in Chile (2010) earthquake as the building code adopted in Chile in 1996 was based on ACI 318-95, except that the boundary element confinement was not required. According to ACI318-11 Equation (21-8), special boundary elements are required for the wall with the minimum horizontal dimension calculated based on the neutral axis depth. The minimum length of confinement was calculated as 1365 mm which is considerably bigger than the 260 mm confinement length of the as-built wall. The confinement reinforcement of the as-built wall did not meet the minimum requirements of ACI318-11§ 21.9.6, and bigger size hoops with smaller spacing were used to satisfy the minimum allowable cross-section area of transverse reinforcement.

According to Eurocode 8, the minimum web thickness is governed by the story height and the minimum boundary thickness is calculated based on the confined length as well as the story height. The existing web thickness of the as-built wall was satisfactory and the confinement length was calculated based on the neutral axis position as well as the required value of the curvature ductility. Since the flexural capacity of the wall was much greater than the flexural demand, the required curvature ductility was reduced resulting in a much smaller value for the confinement length than the ACI318-11 wall section. It should be noted that a bigger value for confinement length required a considerable increase in the minimum boundary element thickness (from 340 mm to 510 mm) and would cause a significant change in the wall section when compared to the sections designed by other codes as well as the as-built wall. Therefore, the minimum confinement length was adopted. The minimum volumetric ratio of confining reinforcement was satisfied using bigger hoop size with smaller spacing. Also, the maximum spacing of the longitudinal reinforcement was limited to 250 mm with cross-ties at every 500 mm connecting two curtains of reinforcement.

Different failure patterns including wall buckling under high axial load, flexural torsional buckling and out-of-plane buckling of the compression zone are addressed in the provisions of NZS3101:2006 for the minimum web and boundary thickness and the effective height to thickness ratio. The as-built wall satisfied the dimensional limitations but did not meet the confinement requirements in plastic hinge region and the modifications were made according to Section 11.4.6.5 of NZS3101:2006.

## 3. Comparative analysis

Nonlinear responses of the four wall models are compared in this section. First, section analysis is carried out to generate the moment-curvature response for each section. Then, the walls are modeled and analyzed in a FEM program to obtain their push-over curves. It should be noted that although the case study wall experienced a 3D out-of-plane failure in the earthquake, only 2D analysis was carried out in this study to evaluate the seismic response of the wall ignoring any possibility of premature out-of-plane instability.

### *3.1 Section analysis*

The major difference between the four wall sections is in the amount and arrangement of transverse hoops because of the different confinement requirements of the design standards. The axial stress-strain curves of the confined concrete obtained using Popovics/Mander`s constitutive model (Mander *et al*. 1988) for the wall sections are compared in Fig. 7(a). The ultimate strain of confined concrete is defined using the equation proposed by Priestley (1996). The stress-strain curve of the as-built configuration is considerably different from the curves of the other sections in terms of both strength and ductility and its ultimate strain is less than half of the strain capacity of the other sections. Fig. 7(b) shows the nonlinear stress-strain curve used for the reinforcing steel.

The moment-curvature curves of the wall sections generated using Xtract (TRC 2011) are shown in Fig. 8 which clearly display the substantial deficiency of the as-built wall in terms of curvature ductility. As expected, the NZS3101 and ACI318 sections with better confinement (the larger amount of hoops and smaller spacing) sustained larger curvature before failure. The

curvature ductility of the Eurocode8 section is higher than the as-built section but substantially less than the NZS3101 and ACI318 sections which is mainly due to its smaller confinement length when compared to the ACI318 and NZS3101 sections. It should be noted that, as shown in Fig. 7(a), the axial stress-strain curve of the confined concrete of the Eurocode8 section (originating from the size and spacing of hoops) indicates a confinement level that is as good as the ACI318 and NZS3101 sections, despite this, the moment-curvature curves of the three wall sections (Fig. 8) are considerably different in terms of curvature ductility; this is mainly due to the difference in the confinement length which has a telling effect on the section behavior.

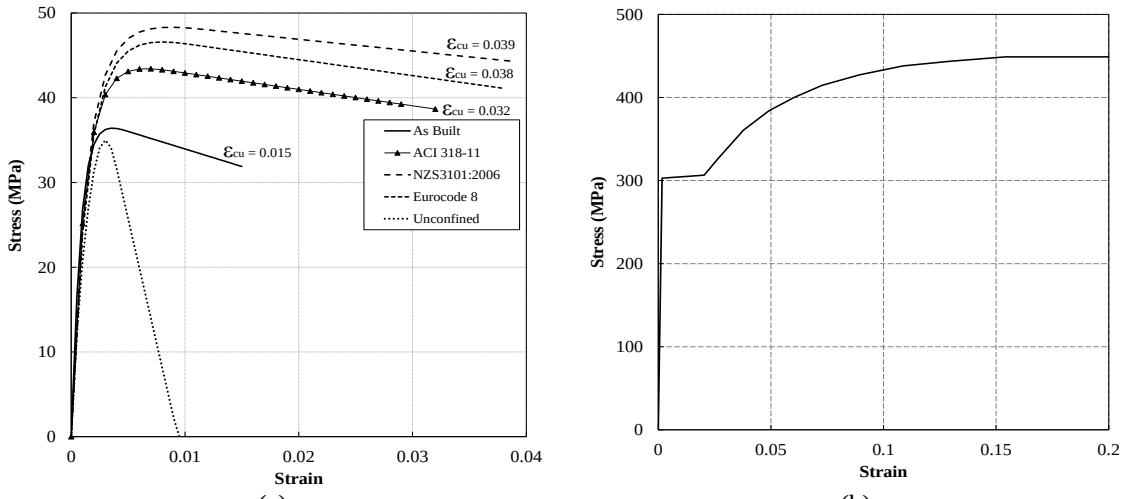


(a) (b)

Fig. 7 (a) Confined concrete models of the wall sections; (b) Stree-strain curve of the reinforcing steel

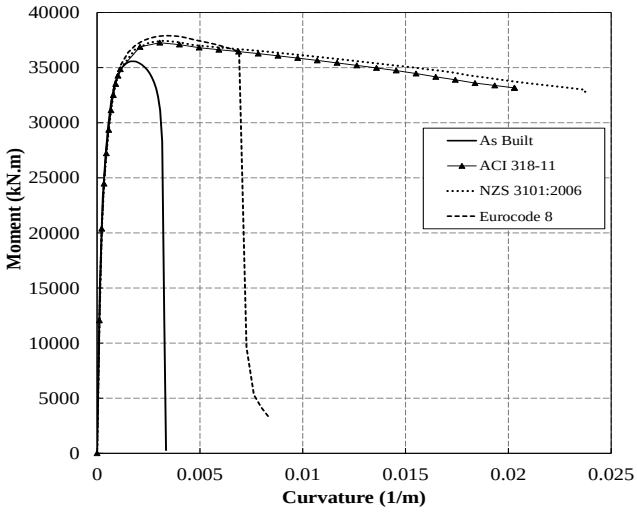


Fig. 8 Moment-curvature curves of the wall sections

### *3.2 Push-over analysis*

In order to capture the push-over curve of the wall sections, the walls are modeled in DIANA9.4.4 (DIANA 2011). Curved shell elements with embedded bar elements are used to simulate the reinforced concrete section (Fig. 9).

The Total Strain Crack Model available in DIANA (DIANA 2011) is used to represent the behavior of the concrete elements. The constitutive model based on total strain is developed along the lines of the Modified Compression Field Theory, originally proposed by Vecchio & Collins (1986). As per the multi-directional fixed crack model, the total strain based crack models follow a smeared approach for the fracture energy. One of the main advantages of this model over other concrete models of DIANA is that basic properties can be derived from Model Code regulations for concrete, or they may be input directly. By default, DIANA assumes appropriate values for the various parameters describing the constitutive behavior.

The axial stress-strain data captured using Popovics/Mander`s constitutive model (Mander *et al*. 1988) (Fig. 10a) is implemented in the Total Strain Rotating Crack model to incorporate the confined concrete properties in the boundary elements and behavior of the unconfined portion is modeled using the axial stress-strain relationship of unconfined concrete.

The reinforcing bars are modelled using Embedded Reinforcement approach available in the program (DIANA 2011). In this approach, reinforcement elements are embedded in structural elements, the so-called mother elements. DIANA ignores the space occupied by the embedded

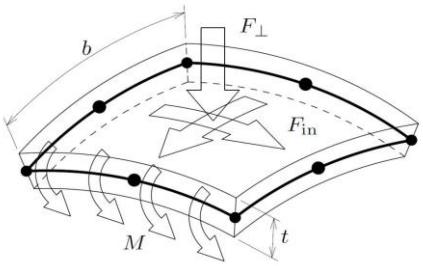


Fig. 9 Curved shell element (DIANA 2011)

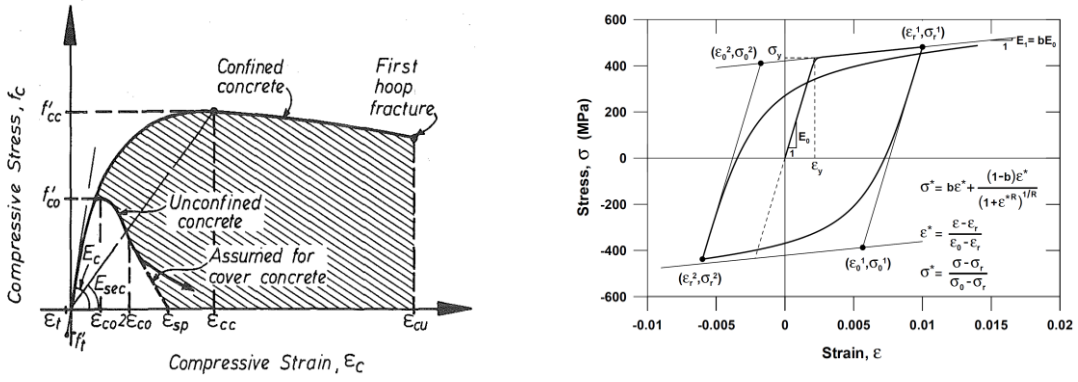


(a) (b)

Fig. 10 Constitutive models of materials: (a) concrete; (b) steel

reinforcing bars. The mother element neither diminishes in stiffness, nor in weight. The reinforcement does not contribute to the weight (mass) of the element. Standard reinforcements do not have degrees of freedom of their own. In standard reinforcement the strains are computed from the displacement field of the mother elements. This implies perfect bond between the reinforcement and the surrounding material. The stress-strain curve of the reinforcing steel is defined using Menegotto and Pinto (1973) model (Fig. 10b). Bar buckling is not included in this constitutive model, hence the effect of bar buckling is neglected in the analysis.

### *3.2.1 Experimental verification*

The finite element model adopted in this investigation is verified using cyclic experimental results of a flexure dominated wall specimen. Specimen RW2 was tested by Thomsen IV and Wallace (1995). A constant axial load of approximately $0.1Agf`_c$was applied to the wall prior to application of the displacement controlled lateral load history. The specimen failed due to bar buckling at 2.5% drift. Fig. 11 displays the geometry and reinforcement details of the specimen as well as schematic view of the finite element model.

Fig. 12 shows a reasonable match between analytical and experimental hysteresis curves. Fig. 13 displays the concrete strain measurements of Specimen RW2 at the wall base in comparison with the model predictions at the positive peak of selected drift cycles applied during testing. The average concrete strains were measured by seven LVDTs over a 229 mm gage length at the base of the wall. The average concrete strain of two consecutive meshes (100 × 100 mm) at the base is

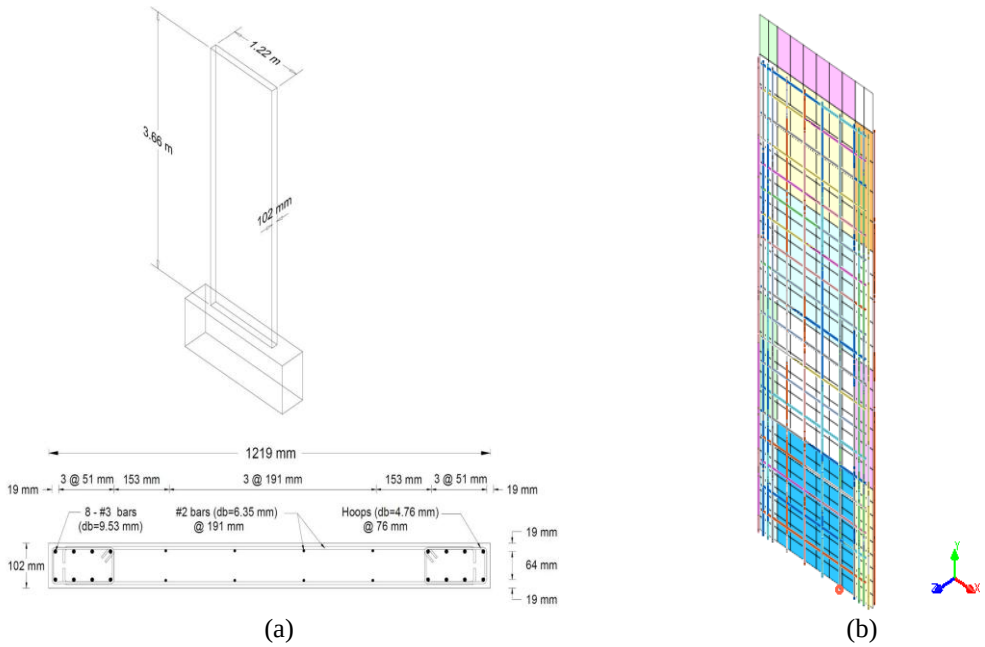


(a) (b)

Fig. 11 Specimen RW2: (a) geometry and reinforcement details (Thomsen IV and Wallace 2004, Orakcal *et al*. 2006); (b) finite element model

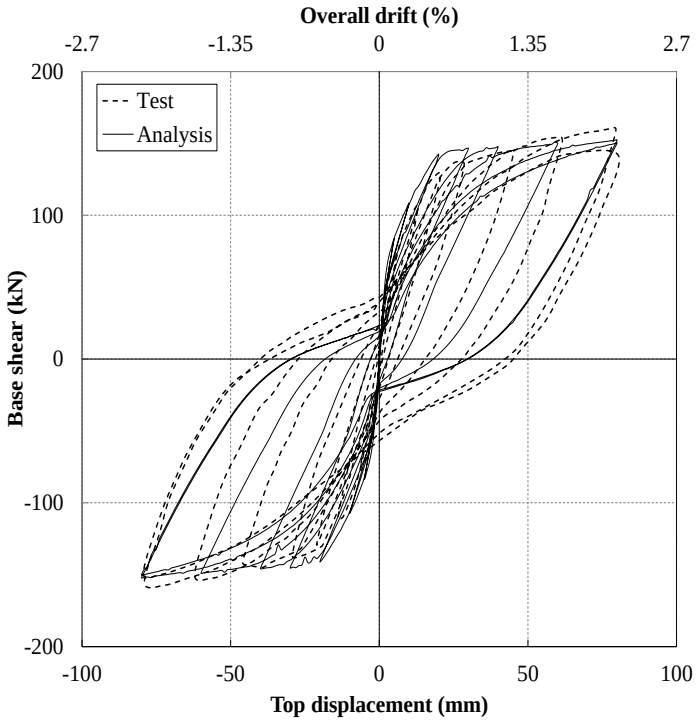


Fig. 12 Lateral load-top displacement response of Specimen RW2

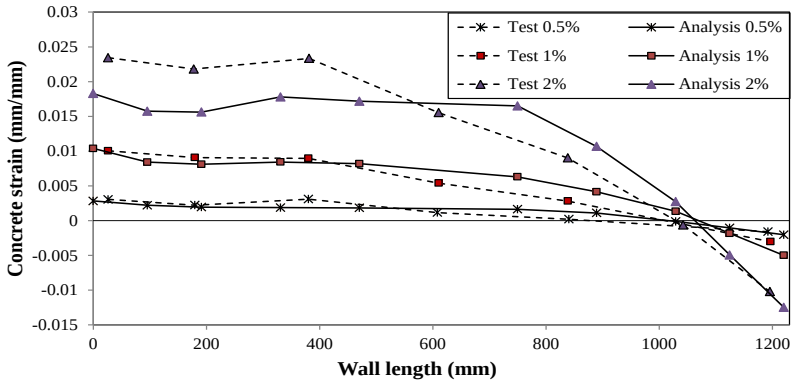


Fig. 13 Wall strain gradient of Specimen RW2

used for comparison. As shown in Fig. 13, the analysis could reasonably predict the strain profile at different drift levels. At the 2% drift level, the difference between the test and analysis is relatively significant although the strain profiles follow the same pattern. The difference at the 2% drift level can be attributed to the bond-slip effect which becomes more influential at higher displacement levels and is not considered in the analysis. Also, the neutral axis position which is one of the main factors in calculating confinement length is well predicted by the analysis. Note that the wall specimen used for verification experienced bar buckling at the ultimate stages of loading. However, the verification shows that the effect of local bar buckling does not

considerably affect the wall response in this case.
used for comparison. As shown in Fig. 13, the analysis could reasonably predict the strain profile at different drift levels. At the 2% drift level, the difference between the test and analysis is relatively significant although the strain profiles follow the same pattern. The difference at the 2% drift level can be attributed to the bond-slip effect which becomes more influential at higher displacement levels and is not considered in the analysis. Also, the neutral axis position which is one of the main factors in calculating confinement length is well predicted by the analysis. Note that the wall specimen used for verification experienced bar buckling at the ultimate stages of loading. However, the verification shows that the effect of local bar buckling does not considerably affect the wall response in this case.

### *3.2.2 Wall models*

The modelling approach described and verified earlier is used for monotonic pushover response evaluation of the redesigned and as-built wall models. The mesh size is chosen based on a mesh sensitivity analysis. The wall models are analyzed using the fine mesh size, which is fine enough to avoid of any mesh size effect (i.e., further reducing the mesh size does not yield any noticeable advantage). Also, the same ratio between element size and wall length was used for the verified specimen. Furthermore, as this study is a comparative investigation, the mesh size is almost identical for all the cases. Out-of plane support is provided at the story levels and a simplified displacement-controlled analysis is carried out with an incremental displacement applied at the top of the wall.

Fig. 14 displays the base shear versus top displacement response of the four walls. As shown in this figure, the as-built wall undergoes a brittle failure when the top displacement is only about 430 mm (i.e., 1.2% average drift). Failure of the Eurocode8 model is also accompanied by sudden degradation of the push-over curve, but the failure displacement is greater than twice of the as-built model. According to the strain profile captured by the analysis the main cause of sudden degradation in these two specimens is reaching the ultimate strain capacity of the concrete elements in the compression side. The models designed based on ACI318-11 and NZS3101:2006 are both ductile enough not to fail within the range of the analyzed displacement (i.e., 2000 mm top displacement or 5.5% average drift). It should be mentioned that reinforcement buckling and bond-slip failure are not considered in these models, although geometric nonlinearity was activated in the analysis to take the P-delta effect into account.

In order to scrutinize the nonlinear response of the wall models at different stages of displacement history, strain profiles along the wall sections as well as the inter-story drift profiles are plotted at some selected points corresponding to considerable changes in the slope of the push-over curves (Figs. 15-18). These key points in the wall response correspond to cracking, yielding of tension and compression reinforcement and the ultimate point. The axial strain profile clearly shows the neutral axis position (corresponding to zero strain) at each stage. The confinement boundary is displayed in each graph to show the neutral axis position with regard to the boundary beyond which the concrete properties change from unconfined to confined or vice versa.

As shown in Fig. 15, at Point A, which corresponds to considerable cracking in the tension side of the wall, the neutral axis position is quite far from the extreme compression fiber which is obviously due to the substantially large axial load ($0.25\, f`_c Ag$). Yielding of the reinforcement at extreme compression and tension fibers start at Points B and C, respectively, resulting in

considerable change of the neutral axis position. The axial load applied to the wall was so great that compression reinforcement yielded before the tension reinforcement. As the axial strain of the unconfined concrete exceeds the strain at the peak stress, strength degrades considerably in sufficient number of concrete elements, which results in overall collapse of the wall. In DIANA, the response of the embedded reinforcement is completely dependent on the mother element which is concrete in this case, and as the mother element becomes unstable, the whole element collapses. At Point D, where the ultimate capacity of the wall is reached, the number of yielded reinforcement is relatively small since the section was not ductile enough to allow much more uniform yielding along the wall length. As shown in Fig. 15, the as-built model could reach the displacement ductility of 1.4 and curvature ductility of 2.01, which is in agreement with the moment-curvature curve plotted in Fig. 8. It should be noted that the strain values at the extreme fibers of the wall section are used for curvature calculations. In other words, as shown in Fig. 15, a linear strain profile is assumed for curvature calculation at ultimate stage ($\varphi$u). The calculated curvatures show good agreement with the results of section analysis which is based on the linear strain profile assumption. The inter-story drift profile of the wall also shows the incapability of the wall to reach an acceptable value of drift.

Fig. 16 indicates the response of the wall designed based on ACI318-11. As previously mentioned, the wall did not fail even at a displacement equivalent to a drift value of 5.5% as the effect of reinforcement buckling and bond-slip was not taken into account. As a consequence, the point corresponding to 80% of the maximum strength of the wall was defined as the ultimate point (Point D). The axial strain versus wall length curve at different points, shown in Fig. 16, displays significant migration of the neutral axis position. Strain profiles corresponding to Points A to C are magnified in the figure to show the neutral axis position at these points. As shown in Fig. 16, the strain values of the ultimate point (Point D) are considerably bigger than the yield point (Point C). In this model the confinement was long enough to protect the unconfined concrete from reaching the peak strength. As shown in Fig. 16, the neutral axis was positioned within the confined concrete zone at the ultimate stage (Point D), where the confinement provided by the transverse reinforcement is enough to ensure a curvature ductility of 17.5 which corresponds to a displacement ductility of 4.2. It should be noted that the ultimate strain of this model at the extreme compression element (0.04) exceeds the ultimate strain value calculated for the confined concrete (0.03). However, the average strain of the mesh element equals 0.03 which is consistent with the calculated value. Also, as mentioned above, the ultimate curvature value (0.014 1/m) is calculated based on the sum of the extreme tension and compression strains divided by the whole length of the wall assuming a linear strain profile and is less than the value captured by the section analysis (Fig. 8), whereas the local curvature at the ultimate point shown in Fig. 16 displays the effect of nonlinear strain profile on the value of curvature ductility. The inter-story drift profile of this model shows its capability to reach a reasonable value of drift at the ultimate point.

The base shear versus top displacement response of the wall designed based on Eurocode8 shows considerable strength degradation at an average drift of 2.6% (Fig. 17). According to the axial strain profile along the wall length, the confinement was not long enough to prevent the unconfined concrete from reaching the peak stress at the ultimate state. The calculated ductility values are 2.9 and 9.6 in terms of displacement and curvature, respectively. Also the value of ultimate curvature is in good agreement with the value obtained from the moment-curvature curve

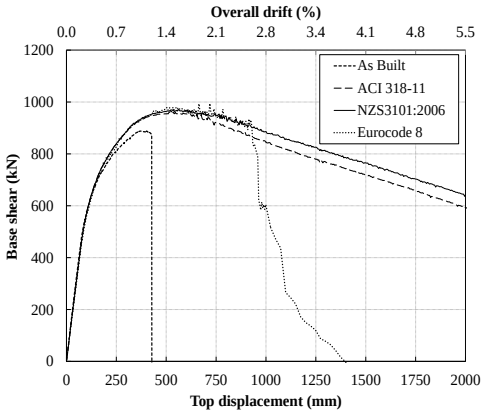


Fig. 14 Base shear-top displacement response of the models

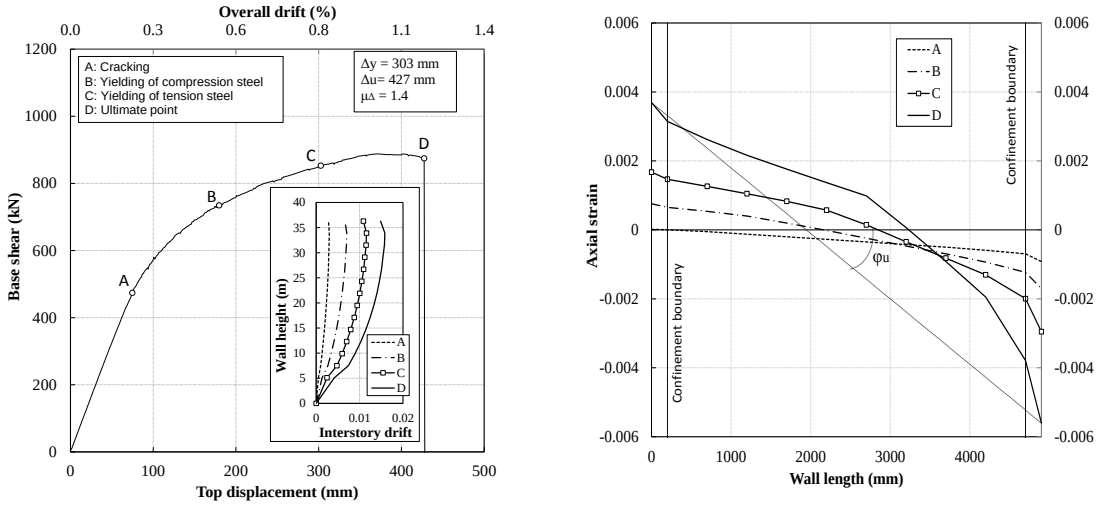


Fig. 15 Push-over response of the as-built model

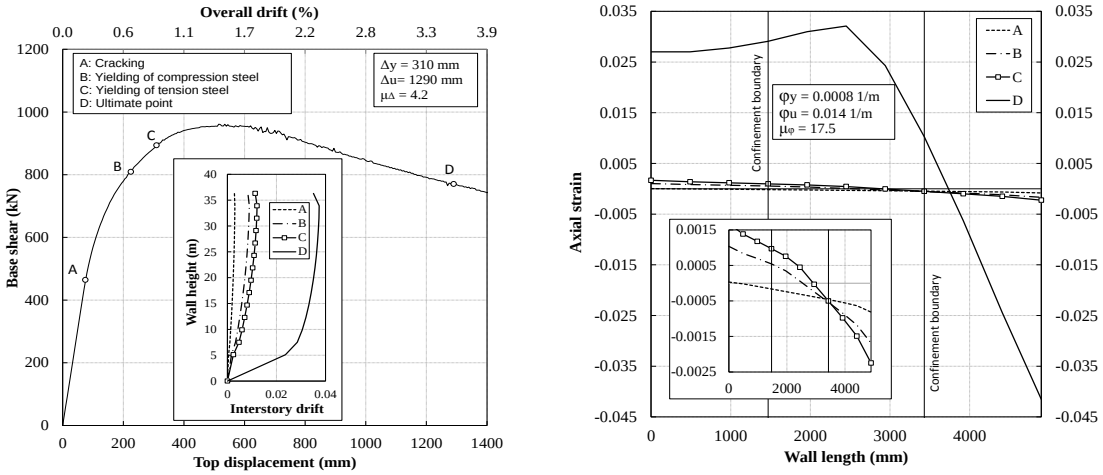


Fig. 16 Push-over response of the ACI318-11 model

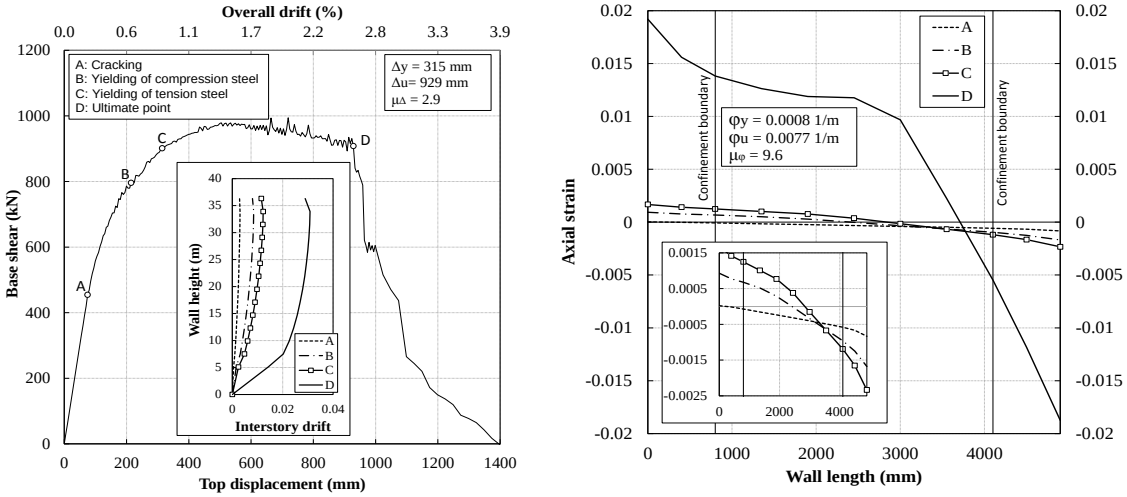


Fig. 17 Push-over response of the Eurocode8 model

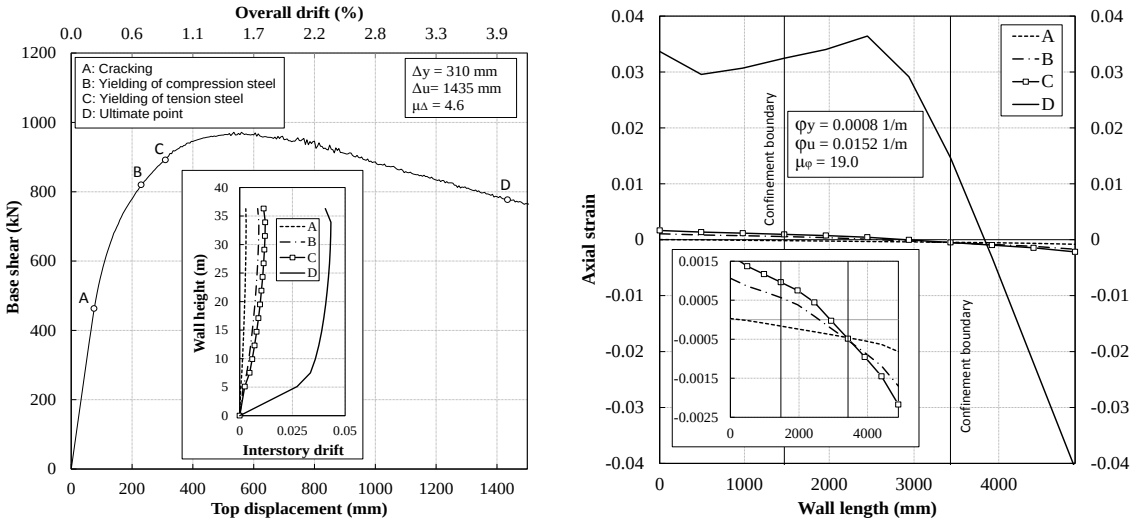


Fig. 18 Push-over response of the NZS3101:2006 model

(Fig. 8). According to Fig. 18, response of the wall designed based on NZS3101:2006 showed a similar trend to the ACI318-11 model. The curvature and displacement ductility values are about 19 and 4.6, respectively, and the wall top displacement at failure (defined as 20% drop in strength) is about 1435 mm, which corresponded to an average drift of about 4.0%.

### *3.3 Confinement length*

In order to investigate the effect of the confinement length on the wall response, the push-over curves of wall models with different confinement lengths are compared. For this purpose, the confinement length of the wall section designed based on ACI318-11 is gradually decreased to

reach the confinement length of the As-Built wall (SW1-SW6, Fig. 19). It should be noted that only the confinement length is changed and the boundary and panel reinforcement configuration are kept the same as the ACI318-11 section.

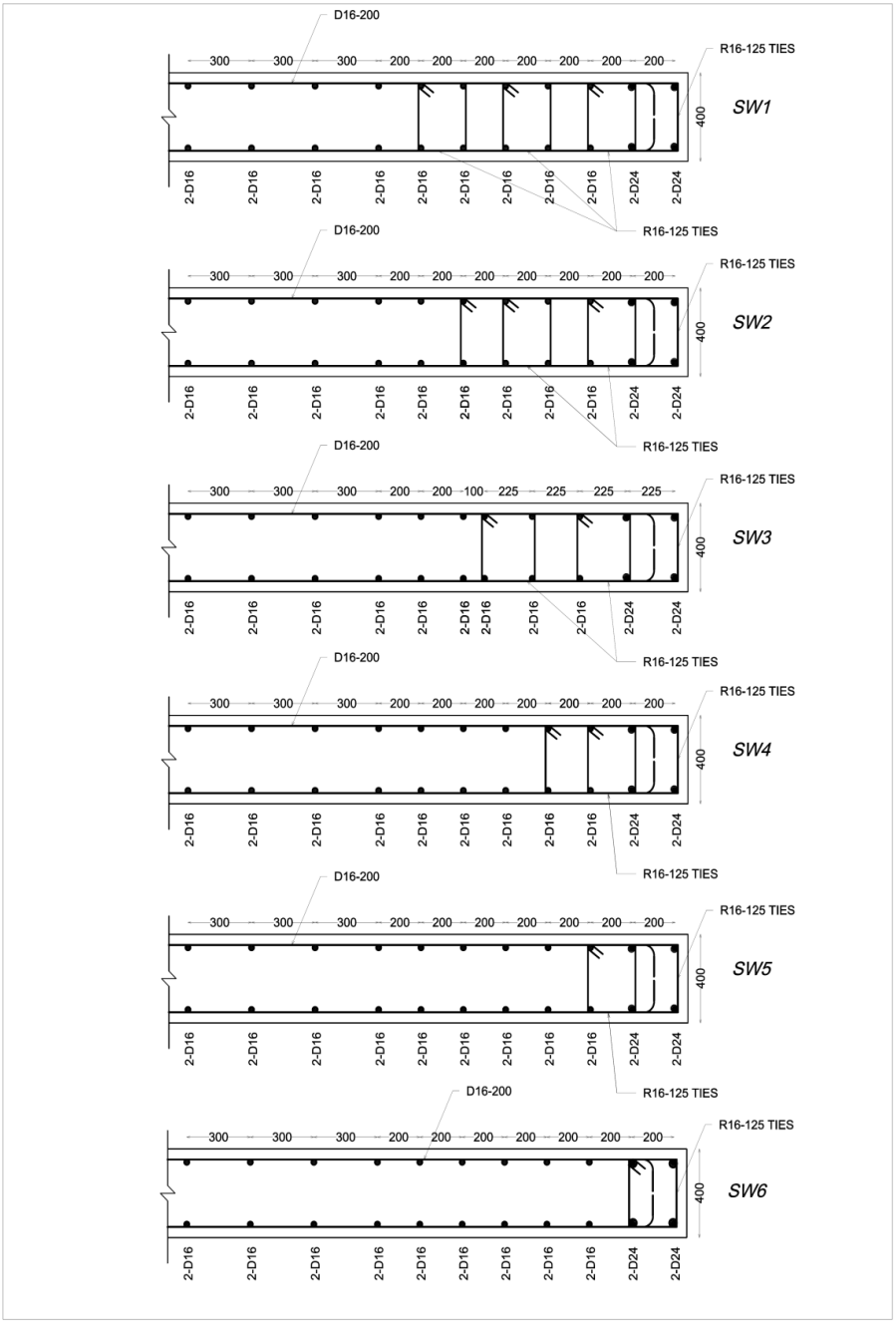


Fig. 19 Wall sections with different confinement lengths

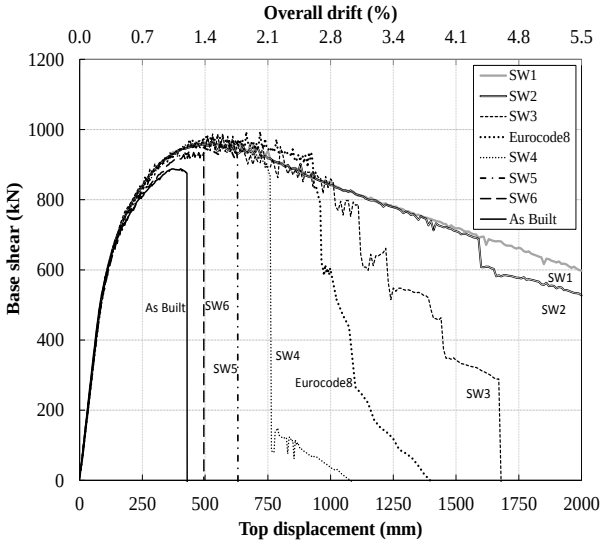


Fig. 20 Push-over curves of the wall sections with different confinement lengths

Fig. 20 ompares the response of the wall models SW1 to SW6 as well as the Eurocode8 and as-built models. The confinement length variation is 200 mm for all models except between SW2 and SW3 where the variation is only 100 mm. Confinement length of the Eurocode8 model is 200 mm smaller than SW2 but its ultimate displacement is much smaller. SW3 shows the sensitivity of the degradation point to the confinement length within the region between SW2 and Eurocode8. Based on the detailed investigation of strain profiles and push-over curves of the different models, the critical confinement length appears to be between SW2 and SW3.

Walls with a confinement length greater than the critical value would have a neutral axis positioned within the confined concrete region when the extreme compression strain exceeds the ultimate strain capacity of confined concrete. The effect of confinement length becomes even more significant at larger axial load ratios. As the axial stress increases, the critical compression strain of unconfined concrete is more likely to reach at smaller values of top displacement. This phenomenon was observed in recent earthquakes. According to Wallace (2012), limit should be placed on the axial stress applied to walls. Higher axial stresses in addition to irregular wall cross section shape (eg. T) in the 2010 Chile earthquake caused concrete compressive strain to reach 0.003 prior to yield of tension steel.

The wall models of ACI318-11 and NZS3101 have such a good confinement that the neutral axis position is within the range of the confinement length at high compression strains resulting in relatively high level of ductility for these models even after reaching 5.5% average drift. However, as the confinement length decreases, the neutral axis position is more likely to be placed outside the confinement length at critical stages of loading. As for SW4, the failure of the wall occurred at 1.8% average drift. SW6 have the same confinement length as the as-built wall but the transverse reinforcement ratio is the one calculated based on ACI318-11. Thus, the confined concrete model is the same as ACI318-11 (Fig. 7(a)) resulting in about 20% increase in displacement ductility compared to the as-built wall.

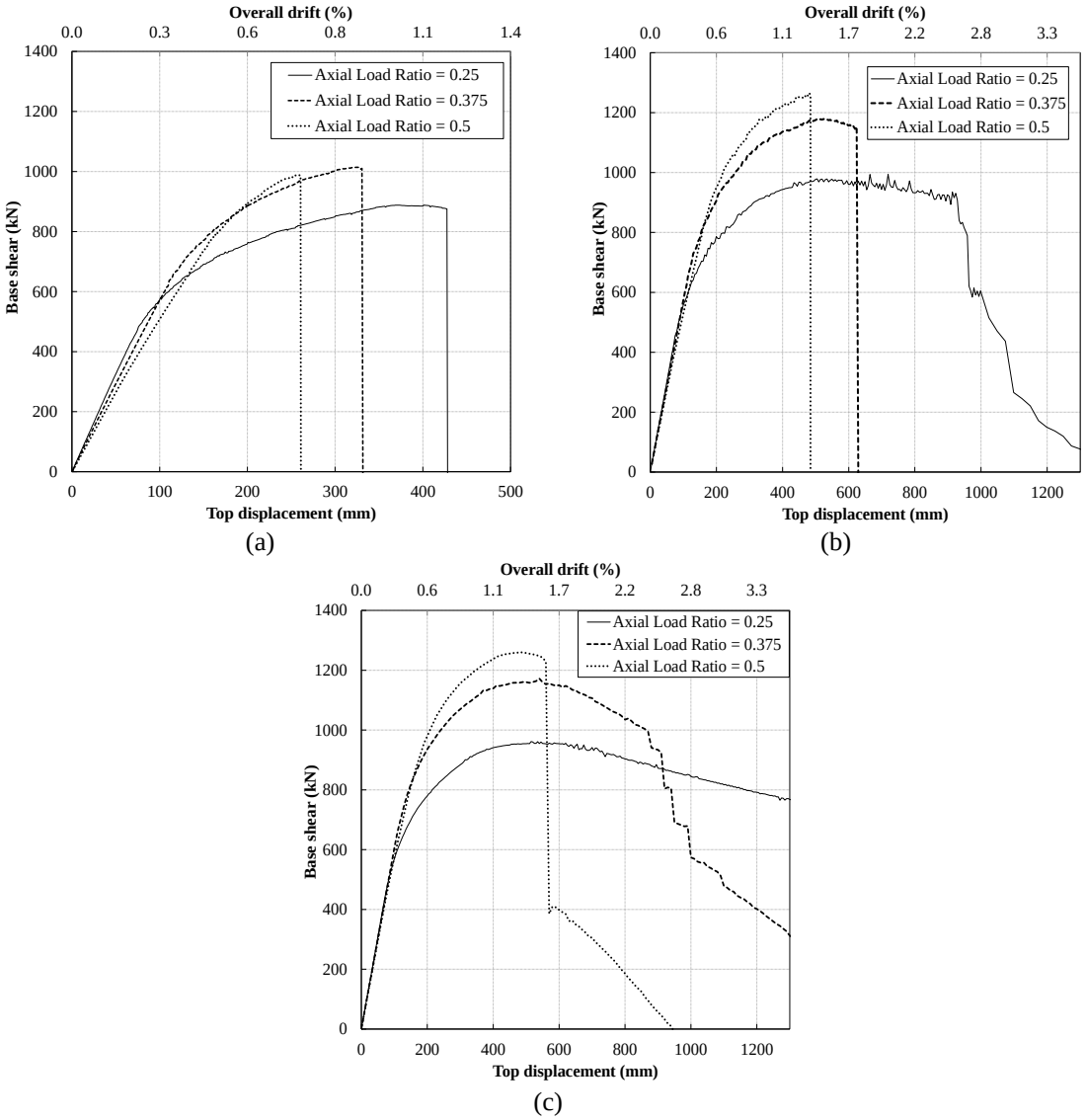


Fig. 21 Effect of axial load ratio on wall response: (a) As-Built wall; (b) Eurocode 8 wall; (c) ACI 318-11 wall

### *3.4 Axial load ratio*

One of the main parameters considerably influencing the response of RC walls is the axial load ratio. According to the reports published on behavior of the Hotel Grand Chancellor in the February Christchurch earthquake, one of the main causes of the wall failure was the considerable underestimation of the axial load ratio used in its design. Also, axial load was amplified during the earthquake because of the constraints and elongation effects (Peng *et al*. 2013). Thus, it is postulated that the damaged wall of the Hotel Grand Chancellor was subjected to a considerably greater axial load than what was taken as the design load. For this purpose, the effect of axial load

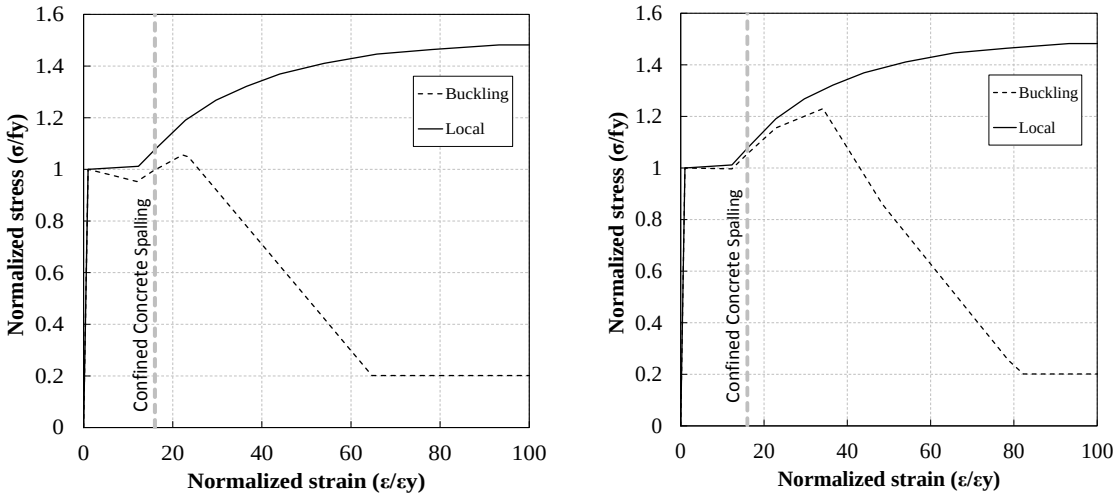


Fig. 22 Postyield buckling of reinforcement: (a) D16; (b) D24

on the push-over response of the wall is investigated herein. The design axial load ratio of the wall is 0.25. The wall models are subjected to 1.5 and 2 times the design axial load. Fig. 21 displays the effect of axial load ratio on the wall`s response. In all cases, increase of the axial load increases the base shear that can be sustained by the wall and significantly decreases the displacement ductility of the section as it forces the section to reach ultimate strain capacity earlier.

### *3.5 Reinforcement buckling*

The effect of bar buckling is not included in the constitutive models used for steel reinforcement in DIANA. However, in order to investigate the effect of bar buckling on wall res ponse, the bar buckling model developed by Dhakal and Maekawa (2002) is used. For this purpose, the axial stress-strain curve of the boundary element bars is extracted from the analysis and compared with the reinforcement strain of the analyzed models. Fig. 22 shows post-yield buckling model of the boundary element reinforcement for the ACI318-11 wall. For all wall models, strain of the compression boundary element at the ultimate point is found to be below the strain corresponding to considerable decrease in the reinforcement capacity due to buckling. Also, embedded reinforcement elements are dependent on the mother elements (concrete in this study) and do not provide any kind of capacity as the corresponding concrete element has reached the spalling strain. The strain corresponding to spalling (i.e., crushing) of the confined concrete is also shown in Fig. 22. As shown in this figure, at this level of section response, consideration of bar buckling has negligible effect on reinforcement response. In other words, the stiffness and spacing of the transverse reinforcement in the boundary elements are enough to prevent buckling of the longitudinal bars before concrete reaches its crushing strain capacity, and in all cases the concrete elements reach the ultimate crushing strain capacity before the reinforcement buckling can have a significant effect on the wall response. However, it should be noted that bar buckling could be influenced by cyclic loading which is not considered in this study.

## 4. Conclusion

The wall D5-6 of the Grand Chancellor Hotel, which was severely damaged in the February 22, 2011 Christchurch earthquake, was designed based on three seismic design codes; ACI318-11, Eurocode 8 and NZS3101:2006. The four wall models were analyzed at section level (moment-curvature analysis) and member level (push-over analysis) and their responses were compared to understand the effect of different design parameters. The base shear versus top displacement responses of the designed walls were captured using DIANA. The strain profiles captured at key points of the wall response such as cracking, yielding of tension and compression reinforcement and the ultimate point were used to scrutinize the nonlinear response of the sections designed based on different codes. All the wall sections responded similarly in terms of the points corresponding to cracking, yielding of compression steel and yielding of tension steel. The large amount of axial load applied to the wall resulted in yielding of the compression reinforcement before the tension reinforcement in all models. However, the ultimate point corresponding to the failure of the wall was quite different in the four models.

The as-built wall model turned out to be unable to sustain displacement and curvature ductility values greater than 1.4 and 2.0, respectively. Redesigning the wall based on ACI 318-11 required a considerably greater confinement length with bigger transverse reinforcement ratio and resulted in a section that could sustain displacement and curvature ductilities of 3.9 and 17.5, respectively. The ultimate point of this model was defined as the point corresponding to the 80% of the peak strength in the post-peak phase as the model did not show any failure up to even 5.5% average drift.

The transverse reinforcement ratio and confinement length of the as-built wall was modified to comply with Eurocode 8, as well. However, as the required confinement length based on Eurocode 8 was less than that for ACI318-11, The Eurocode8 wall model sustained a brittle failure at about 2.6% overall drift with displacement and curvature ductility values of 2.9 and 9.6, respectively.

The confinement requirements of NZS3101:2006 resulted in a section that was almost the same as ACI318-11 wall model and the only difference was a smaller value of the transverse reinforcement spacing. As a consequence, the displacement and curvature ductility values captured by the NZS3101 section were slightly greater; i.e., 4.5 and 19, respectively.

The curvature values calculated by the strains at the extreme fibers captured by the FEM and assuming linear strain profile was in good agreement with the moment-curvature diagram derived from section analysis while the nonlinear strain profile shows a relatively bigger curvature.

A parametric study was carried out to further investigate the effect of confinement and axial load ratio on the ultimate drift capacity. The confinement length effectively determines the maximum displacement that the wall can undergo without brittle failure of the unconfined concrete. The increase in axial load ratio considerably affected the response of the wall models, and resulted in slight increase in strength but considerable decrease in ductility capacity of well confined walls.

Although providing a good level of confinement using larger amount of hoops with smaller spacing increases the strength and ductility of the wall section, the confinement length plays a key role in the lateral nonlinear in-plane response of RC walls. For example, a section with enough volumetric ratio of transverse reinforcement provided within a smaller length than a critical value is likely to experience an abrupt strength degradation before reaching an acceptable value of displacement as well as curvature ductility.

The case study wall experienced a 3D out-of-plane failure in the earthquake. However results of the 2D analysis revealed the fact that even without any trigger for 3D overall failure, the wall would not have been able to sustain the drift demand and would fail in a brittle manner. On the other hand, it was found that improved detailing, as required by the modern concrete codes, would have ensured a ductile in-plane response of the walls if the out-of-plane stability was ensured.

## References

ACI318 (2011), Building Code Requirements for Structural Concrete (ACI 318-11) and Commentary (ACI318R-11). American Concrete Institute, Farmington Hills, Michigan.

Boulanger, B., Paultre, P. and Lamarche, C.P. (2013), "Analysis of a damaged 12-storey frame-wall concrete building during the 2010 Haiti earthquake - Part II: Nonlinear numerical simulations", *Can. J. Civ. Eng.*, **40**(8), 803-814.

CEN, C. E. d. N. (2004), "Eurocode 8: Design of structures for earthquake resistance", Part 1, 1998-1991.

Dhakal, R. and Maekawa, K. (2002), "Modeling for Postyield Buckling of Reinforcement", *J. Struct. Eng.*, **128**(9), 1139-1147.

DIANA, T. (2011), Finite Element Analysis User's Manual - Release 9.4.4, TNO DIANA.

Dunning Thornton Report (2011), *Report on the Structural Performance of the Hotel Grand Chancellor in the Earthquake of 22 February 2011. Report for the Department of Building & Housing. http://www.dbh.govt.nz/userfiles/File/Reports/quake-structural-performance-hotel-grand-chancellor.pdf*, Dunning Thornton Consultants Ltd.

EERI (2011), *The M 6.3 Christchurch, New Zealand, Earthquake of February 22*, EERI Special Earthquake Report.

Elwood, K.J. (2013), "Performance of concrete buildings in the 22 February 2011 Christchurch earthquake and implications for Canadian codes 1", *Can. J. Civ. Eng.*, **40**(3), 1-18.

Kam, W. Y., S. Pampanin and K. Elwood (2011), "Seismic performance of reinforced concrete buildings in the 22 February Christchurch (Lyttelton) earthquake", *Bull. New Zealand Soc. Earthq. Eng.*, **44**(4), 239-278. J R SOC NEW ZEAL

Luu, H., Ghorbanirenani, I., Leger, P. and Tremblay, R. (2013), "Numerical modeling of slender reinforced concrete shear wall shaking table tests under high-frequency ground motions", *J. Earthq. Eng.*, **17**(4), 517-542.

Mander, J., Priestley, M.N. and Park, R. (1988), "Theoretical stress-strain model for confined concrete", *J. Struct. Eng.*, **114**(8), 1804-1826.

Massone, L.M., Orakcal, K. and Wallace, J.W. (2009), "Modeling of squat structural walls controlled by shear", *ACI Struct. J.*, 106(5).

Menegotto, M. and Pinto, P. (1973), Method of Analysis for Cyclically Loaded Reinforced Concrete Plane Frames Including Changes in Geometry and Non-elastic Behavior of Elements Under Combined Normal Force and Bending. IABSE Symposium on the Resistance and Ultimate Deformability of Structures Acted on by Well-Defined Repeated Loads, Lisbon.

NZRC (2012), *Canterbury Earthquakes Royal Commission Reports*, http://canterbury.royalcommission.govt.nz/Final-Report-Volume-Two-Contents.

NZS3101 (2006), NZS 3101:2006 Concrete Structures Standard. Part 1: The Design of Concrete Structures.

Orakcal, K., Massone, L.M. and Wallace, J.W. (2006), "Analytical modeling of reinforced concrete walls for predicting flexural and coupled-shear-flexural responses", Pacific Earthquake Engineering Research Center, College of Engineering, University of California, Berkeley.

Panagiotou, M., Restrepo, J.I., Schoettler, M. and Kim, G. (2012), "Nonlinear cyclic truss model for reinforced concrete walls", *ACI Struct. J.*, **109**(2), 205-214.

Peng, B., Dhakal, R., Fenwick, R., Carr, A. and Bull, D. (2013), "Multispring hinge element for reinforced

concrete frame analysis", *J. Struct. Eng.*, **139**(4), 595-606.
Priestley, M. N. (1996), Seismic design and retrofit of bridges, Wiley-Interscience.
Song, W., Dyke, S. and Harmon, T. (2013), "Application of nonlinear model updating for a reinforced concrete shear wall", *J. Eng. Mech.-Asce*, **139**(5), 635-649.
Sullivan, T.J. (2010), "Capacity design considerations for RC frame-wall structures", *Earthq. Struct.*, **1**(4), 391-410.
Telleen, K., Maffei, J., Heintz, J. and Dragovich, J. (2012a), "Practical lessons for concrete wall design, Based on studies of the 2010 chile earthquake", *15th World Conference on Earthquake Engineering, 24-28 September 2012*, Lisbon, Portugal.
Telleen, K., Maffei, J., Willford, M., Aviram, A., Huang, Y., Kelly, D. and Bonelli, P. (2012b), Lessons for Concrete Wall design from the 2010 Maule Chile Earthquake, *Proceedings of the International Symposium on Engineering Lessons Learned from the 2011*, Great East Japan Earthquake, March 1-4, 2012, Tokyo, Japan.
Thomsen IV, J.H. and Wallace, J.W. (1995), *Displacement-Based Design of Reinforced Concrete Structural Walls: An Experimental Investigation of Walls with Rectangular and T-Shaped Cross-Sections*, Report No. CU/CEE-95-06, Department of Civil and Environmental Engineering, Clarkson University, Potsdam, N.Y.
Thomsen IV, J.H. and Wallace, J.W. (2004), "Displacement-based design of slender reinforced concrete structural walls-experimental verification", *J. Struct. Eng.*, **130**(4), 618-630.
TRC (2011), XTRACT, Imbsen Software Systems, 9912 Business Park Drive, Suite 130, Sacramento, CA 95827.
Vecchio, F.J. and Collins, M.P. (1986), "The modified compression-field theory for reinforced concrete elements subjected to shear", *ACI J.*, **83**(2), 219-231.
Wallace, J. (2012), "Behavior, design, and modeling of structural walls and coupling beams — Lessons from recent laboratory tests and earthquakes", *Int. J. Concrete Struct. Mater.*, **6**(1), 3-18.
Wallace, J. and Moehle, J. (2012), "Behavior and design of structural walls-Lessons from recent laboratory tests and earthquakes", *Proceedings of the International Symposium on Engineering Lessons Learned from the 2011 Great East Japan Earthquake*, March 1-4, 2012, Tokyo, Japan.
Wan, H. and Li, P. (2012), "Finite element simulation of RC shear wall components", Progress in Civil Engineering, Pts 1-4.
Chu, M.J., Li, X.G., Lu, J.Z., Hou, X.M. and Wang, X., Amsterdam, Elsevier Science Bv. 170-173, 3594-3597.